Heat Mass Transfer (2013) 49:299–308
DOI 10.1007/s00231-012-1086-7

ORIGINAL

Sensitivity analysis of thermal design parameters for focal plane assembly in a space spectral imaging instrument

Liang Guo · Qing-wen Wu · Chang-xiang Yan

Received: 20 December 2011 / Accepted: 10 October 2012 / Published online: 31 October 2012

Abstract There are deviations between real parameters and thermal design parameters on thermophysical attribute of focal plane assembly (FPA). The parameters are difficult to be determined accurately and the thermal design scheme will be affected with the values of the parameters. The thermal design problem of FPA is described by means of system sensitivity theory. The in-orbit heat balance equations are established, and the thermal design parameters, which might affect the temperature distribution of the FPA, are given. As an example, the sensitivity of thermal design parameters is analyzed for a FPA in a space spectral imaging instrument. A basis to determine the structural and thermophysical parameters for FPA is gotten, furthermore, an analytical method is provided for reliability validation of thermal design and operating reliability on orbit. It is shown that contact heat-transfer coefficient between mounted surfaces and surface emissivity are the main parameters affecting mean temperature of Charge converse device (CCD). The power of the inner heat source, thermal conductivity and inner contact heat-transfer coefficient are the primary parameters affecting temperature difference between CCD and the heat-transfer block. The thermal test is set up, and it is illuminated that the sensitivity analysis strategy based on the thermal design scheme is effective and feasible.

L. Guo (✉) · Q. Wu · C. Yan
Changchun Institute of Optics, Fine Mechanics and Physics, Chinese Academy of Sciences, Changchun 130033, Jilin, China
e-mail: guoliang329@hotmail.com

Q. Wu
e-mail: wuqw@ciomp.ac.cn

C. Yan
e-mail: yancx@ciomp.ac.cn

L. Guo
Graduate School of Chinese Academy of Sciences, Beijing 100039, China

1 Introduction

The resolution of space optics remote sensor has been increasing continuously along with the development of modern science, technology and the requirement for great amount of information. Heat generated at focal plane assembly (FPA) in space optics remote sensor is becoming more and more. The advancement of imaging performance and reliability is limited greatly due to the heat elimination problem of FPA [1, 2]. At the present time, thermal design and thermal control technology for FPA is a key section of thermal control system for the space optics remote sensor [3–9].

Sensitivity analysis is suitable to settle the optimum design problems with multivariable and complex mathematical model, and it would be an important significance on engineering application. The design parameter sensitivity is the differential information for the design parameters of the system state, which might reflect the trend and degree of changes. There is a comprehensive application at optimum design, failure mode evaluation analysis, indirect problem and so on [10–12]. The thermal design parameters include the power of inner heat source, surface emissivity, etc. Thermal design parameter sensitivity is computed to disclosure the influence of thermal design parameters on temperature distribution; furthermore, it is the key information to find the optimum thermal design proposal.

Sensitivity analysis in temperature field has been studied by researchers all over the world, such as comprehensive researches on the continuation of original research technique [13–17], the exploitation of new computational model

[18–20], and the introduction to new application field [21–24] and so on. In order to investigate the thermo-optical properties of space optics remote sensor, temperature field of optical window in manned spacecraft is discussed with the sensitivity analysis method, and the influence on thermo-optical error of optical window is deduced due to the variational temperature level, the axial temperature difference, the radial temperature difference and the circumferential temperature difference [25, 26]. The curves fitting to the data of image quality analysis for a typical R–C imaging system's primary optical equipment is achieved with the help of the sensibility analysis method. Hereby, some suggestions for the temperature control of the imaging system are put forward [27]. Thermal design parameter sensitivity analysis could guide thermal design effectively. The thermal design problem of the satellite is analyzed by means of the theory of the system sensitivity analysis and the system sensitivity equations are derived for the thermal design of a satellite. As an example, the system sensitivity equations are applied to the parameter sensitivity analysis of thermal design for the solar array and the sensitivity of each design parameter is discussed [28, 29]. The temperature sensitivity and infrared radiation sensitivity formulae of surface node belonged to a satellite were derived, according to the calculation model of temperature and infrared radiation. Combined with specific satellite's parameters, the temperature sensitivity and infrared radiation sensitivity were calculated [30]. However, there is not a comprehensive analysis on thermal design parameters in those papers mentioned above, especially internal thermal design parameters (such as inner heat conduction) and external thermal design parameters (such as contact heat-transfer coefficient for the mounted surfaces) are not discussed. Sensitivity analysis of the contact conduction and the position of thermostat on the basis of thermal model established are performed, and the study of thermal design is accomplished for the preparation of possible mechanical interface change of the satellite propulsion system depending on the design of a satellite system [31]. Based on the results from the validated model, the heat loss, the positions of the temperature sensors, the input power, and the heater length is investigated. The sensitivity of the thermal parameters is stated [32]. The sensitivity and uncertainty of heat exchanger designs to physical properties estimation have been studied with Monte Carlo methods. The analysis method could be used to identify when and which, properties play a significant role in the error propagation for this type of equipment [33]. On the basis of a sensitivity study, a numerical study is conducted to evaluate the potential for using wellbore heat exchangers (WBHX) to extract heat in electricity generation. The variable parameters studied included operational parameters such as wellbore geometries, working fluid properties, circulation rates, and regional properties including basal heat flux and formation rock type [34]. The internal thermal design parameters (such as inner heat conduction) and external thermal design parameters (such as contact heat-transfer coefficient for mounted surfaces) both affect the mean temperature of FPA. Therefore, all the internal and external thermal design parameters should be all discussed for its sensitivity analysis. Comparing with the papers mentioned above, more detailed and more comprehensive sensitivity analyses on thermal design parameters of FPA are discussed in this paper, and the inner heat conduction and contact heat-transfer coefficient for mounted surfaces is paid much attention to.

In the space environment, some thermal design parameters are unable to be confirmed accurately in the course of thermal design and thermal analysis for the FPA. To identify when and which, thermal design parameters play a significant role in the temperature field for the FPA; the thermal design parameter sensitivity analysis is necessary. The pertinence and validity of thermal design can be enhanced through sensitivity analysis. Furthermore, sensitivity analysis could improve work efficiency, reduce cost and increase reliability. As an application of sensitivity analysis method, the thermal design parameters sensitivity is discussed for a FPA in space spectral imaging instrument with software IDEAS-TMG. Inner heat source, material thermal conductivity, inner contact heat-transfer coefficient, contact heat-transfer coefficient for mounted surfaces, and surface emissivity are included for thermal design parameters sensitivity analysis. The aim is to supply theoretical support for determining thermal and structural parameters for a FPA of space optics instrument. The thermal design parameters sensitivity analysis is suitable to increase reliability for thermal system of FPA.

2 Thermal equilibrium equations and design variables analysis

2.1 Thermal equilibrium equations

The temperature of FPA depends on environment condition and its thermal properties [35]. Thermal equilibrium in surrounding environment for FPA is shown in Fig. 1. According to conservation of energy principle, thermal analysis model is established with the thermal equilibrium equations for FPA and its surrounding environment. The thermal equilibrium equations are given bellow:

$$\begin{cases} Q_1 + Q_2 = Q_3 + Q_4 + Q_5 \\ Q_1 = \sum q_i \\ Q_2 = \sum H_{ij}(T_i - T_j) + \sigma \sum \varepsilon_{kl} \Phi_{kl} A_{kl} (T_k^4 - T_l^4) \\ Q_3 = \sum H_{fm}(T_{fp} - T_{ms}) \\ Q_4 = \sum \left(m_k c_k \frac{\partial T}{\partial \tau} \right) \\ Q_5 = \sigma \sum \varepsilon_{fp} \Phi_{fp} A_{fp} (T_{fpe}^4 - T_{ee}^4) \end{cases} \quad (1)$$

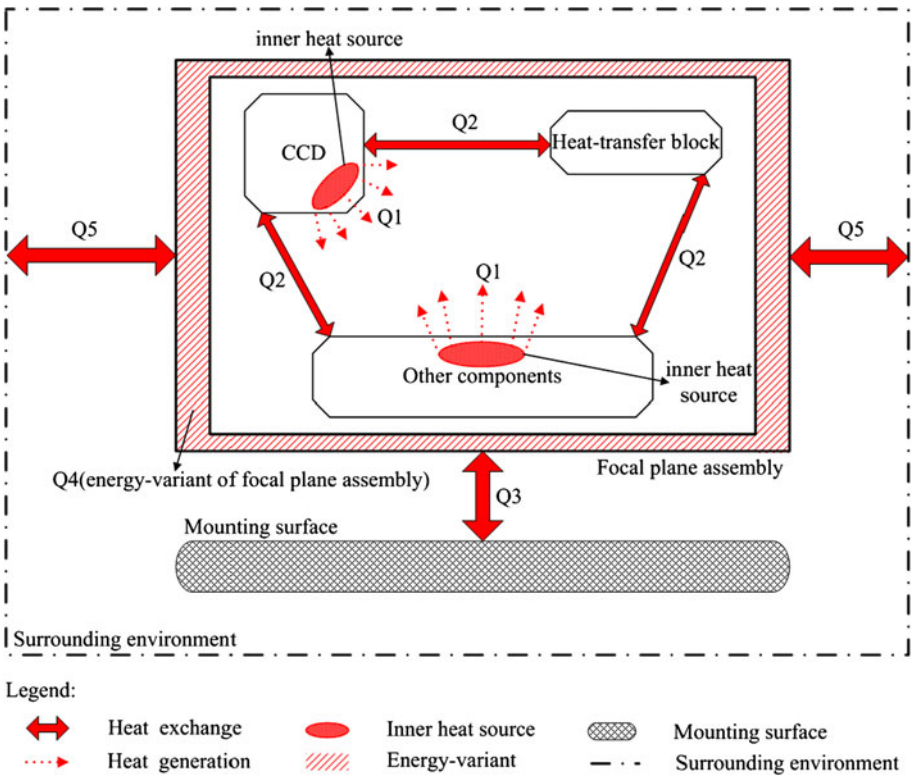

Fig. 1 Thermal equilibrium in surrounding environment for FPA

Table 1 Variables affecting temperature distribution

No.	Items	Design variables analysis
1	The heat productivity from inner heat source in FPA: q_i	Adjustable, belong to thermal design variables
2	Conductivity factor between inner elements in FPA: H_{ij}	Adjustable, belong to thermal design variables
3	Surface emissivity of inner elements in FPA: ε_{kl}	Unadjustable, determined by structural and optical design
4	Conductivity factor between FPA and mounting surface: H_{fm}	Adjustable, belong to thermal design variables
5	Radiation factors between inner elements in FPA: Φ_{kl}	Unadjustable, determined by structural and optical design
6	Effective area of inner elements in FPA which taking part in radiation heat exchange: A_{kl}	Unadjustable, determined by structural and optical design
7	Mass of inner elements in FPA: m_k	Unadjustable, determined by structural material
8	Thermal capacity of inner elements in FPA: c_k	Unadjustable, determined by structural material
9	Surface emissivity of FPA: ε_{fp}	Adjustable, belong to thermal design variables
10	Radiation factor between FPA and surrounding environment: Φ_{fp}	Unadjustable, determined by structural design
11	Effective area of FPA surface which taking part in radiation heat exchange: A_{fp}	Unadjustable, determined by structural design

where Q_1 is the power of the inner heat source of FPA; q_i is the power from each chip of FPA; Q_2 is exchanged power between inner heat source and the other components; i, j are the elements with contact thermal conduction relation; k, l are the elements with radiation thermal conduction relation; H_{ij} is conductivity factor between inner elements in FPA; σ is Boltzmann constant, $\sigma = 5.67 \times 10^{-8}\ \mathrm{W}/\left(\mathrm{m}^2\ \mathrm{K}^4\right)$; T_i, T_j, T_k, T_l are temperature of inner elements in FPA; ε_{kl} is surface emissivity of inner elements in FPA; Φ_{kl} is radiation factors between inner elements in FPA; A_{kl} is equivalent area of inner elements in FPA which taking part in radiation heat exchange; $Q3$ is the power of thermal conduction between FPA and mounting surface; H_{fm} is conductivity factor between FPA and mounting surface; T_{fp}, T_{ms} are temperature of FPA and mounting surface; Q_4 is the power of energy-variant of FPA; m_k is mass of inner elements in FPA; c_k is thermal capacity of inner elements in FPA; $\frac{\partial T}{\partial \tau}$ is rate of variation in temperature

of FPA; Q_5 is the power of radiation between FPA and surrounding environment; ε_{fp} is surface emissivity of FPA; Φ_{fp} is radiation factor between FPA and surrounding environment; A_{fp} is equivalent area of FPA surface which taking part in radiation heat exchange; T_{fpe}, T_{ee} a temperature of FPA surface and surrounding environment.

2.2 Design variables analysis

From the equations given above, variables which influence temperature distribution of FPA are given in Table 1.

During thermal design process for FPA, some design variables could influence temperature distribution strongly, such as the heat productivity from inner heat source in FPA q_i, conductivity factor between inner elements in FPA H_{ij}, conductivity factor between FPA and mounting surface H_{fm} and surface emissivity of FPA ε_{fp}.

3 Sensitivity analysis

3.1 Structural and thermal model [2]

The cross-sectional view of FPA structure is shown in Fig. 2. The heat generated from CCD is transferred to the enclosure of heat-transfer block.

According to structure given above, heat transfer channel could be determined. By means of reasonable preprocess and equivalent treatment, the thermal model is given with IDEAS-TMG as shown in Fig. 3.

Different boundary condition such as inner heat source, conductivity factor, thermal conductivity, and surface emissivity is set in the analysis model, and the sensitivity of each variable which could influence temperature distribution of FPA is given through numeric computation.

3.2 Variation of the heat from inner heat source

During development process of FPA, there are different extent improvement and optimization for parameters such as heat generation and distribution. These changes will bring variation of temperature distribution. Thereby, it is necessary to discuss the influence on temperature distribution of FPA induced by variation of the heat generation from inner heat source.

During computation process, the power of CCD is set to be different number as shown in Table 2. At the same time, the power of drive unit also augments with the increasing power of CCD. The other computational parameters are constant.

The effect of the power of inner heat source on mean temperature of FPA is shown in Fig. 4. The mean temperatures of CCD and heat-transfer block goes up near-linearly as increasing power of inner heat source.

The sensitivity of inner heat source on mean temperature in FPA is shown in the Fig. 5. The sensitivity of inner heat source on mean temperature of CCD and heat-transfer block is 3.8–3.9 °C/W and 1.25–1.35 °C/W, respectively. Comparing with heat-transfer block; CCD is influenced greater by the inner heat source. Thereby, under the condition with definite thermal resistance along heat transfer channel, the temperature of CCD is faster than that of heat-transfer block because of the increasing inner heat source.

3.3 Variation of inner heat conduction

Two parts for inner heat conduction in FPA will be discussed. They are thermal conductivity of material and inner contact heat-transfer coefficient between interfaces.

Commonly, the frame material of electron device on orbit is aluminum alloy or magnesium alloy. The order of

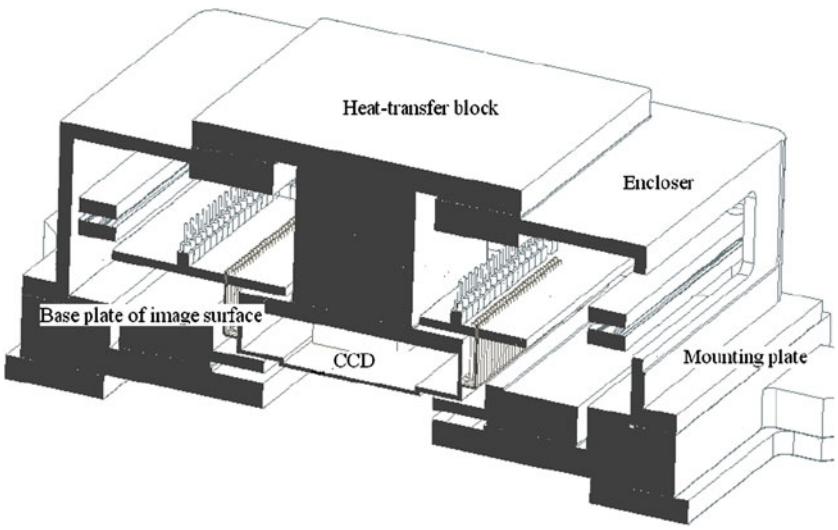

Fig. 2 Cross-sectional view of FPA structure

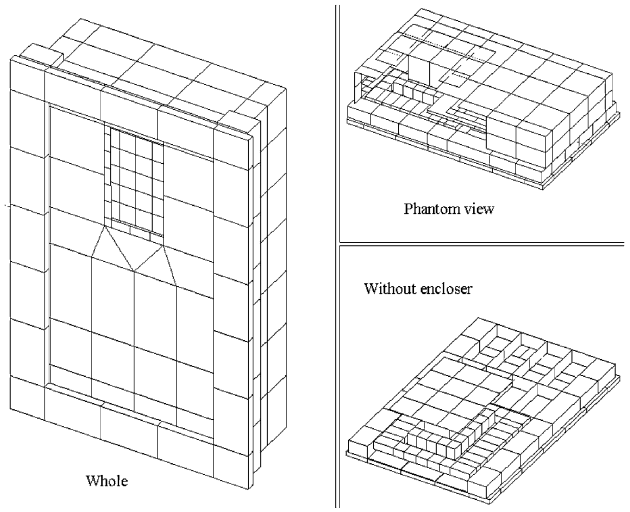

Fig. 3 Thermal model of FPA

magnitude for thermal conductivity is 10 W/(mK)–10^2 W/(mK). Thereby, during computation process, the material thermal conductivity of frame material is set to be different number as shown in Table 2. Other computational parameters maintain constant.

The effect of material thermal conductivity on mean temperature of FPA is shown in the Fig. 6.

Thermal resistance along heat transfer channel in composed of thermal resistance inside of material and thermal contact resistance between interfaces. Under the circumstances, the thermal resistance inside of material decreases gradually as increasing material thermal conductivity. The mean temperature of CCD and heat-transfer block reduces gradually as increasing material thermal conductivity because of the reduction of thermal resistance along heat transfer channel. The temperature uniformity and heat-sinking capability of FPA are improved as the increasing of material thermal conductivity.

The sensitivity of material thermal conductivity on mean temperature in FPA is shown in the Fig. 7.

As shown in the Fig. 7, the sensitivity of material thermal conductivity on mean temperature of CCD and heat-transfer block is -7.5×10^{-3} m °C^2/W to -4.3×10^{-2} m °C^2/W and -5×10^{-3} m °C^2/W to -3.5×10^{-2} m °C^2/W, respectively. The sensitivity of material thermal conductivity on CCD is higher than heat-transfer block. Under the circumstances, the temperature of CCD is influenced more strongly with the material thermal conductivity than heat-transfer block.

According to the requirement for thermal control on inner elements in FPA, there is heat-conducting processing mode between interfaces. The order of magnitude for inner contact heat-transfer coefficient is 10^2 W/(m^2 K)–10^3 W/(m^2 K). Thereby, during computation process, the inner contact heat-transfer coefficient between interfaces is set to be different number; inner contact heat-transfer coefficient parametric variations are given in Table 2. Other computational parameters maintain constant.

The effect of inner contact heat-transfer coefficient on mean temperature of FPA is shown in the Fig. 8.

Thermal resistance along heat transfer channel is composed of thermal resistance inside of material and thermal contact resistance between interfaces. Under the circumstances, the thermal contact resistance between interfaces decreases gradually as increasing inner contact heat-transfer coefficient. As shown in the Fig. 8, the mean temperature of CCD and heat-transfer block fall down gradually as the increasing of inner contact heat-transfer coefficient

Table 2 Parametric variations

Items	First calculation	Second calculation	Third calculation	Fourth calculation	Fifth calculation	Sixth calculation	Seventh calculation	Eighth calculation	Ninth calculation	Tenth calculation
Power [W]	1	2	3	4	5	6	7	8	9	10
Thermal conductivity of frame material [W/(mK)]	70	100	120	140	160	180	200	220	240	–
Inner contact heat-transfer coefficient [W/(m^2 K)]	100	300	500	700	900	1,100	1,300	1,500	2,000	–
Contact heat-transfer coefficient between mounted surfaces [W/(m^2 K)]	10	50	100	300	500	700	900	1,200	1,500	2,000
Surface emissivity	0.05	0.15	0.25	0.35	0.45	0.55	0.65	0.75	0.85	0.95

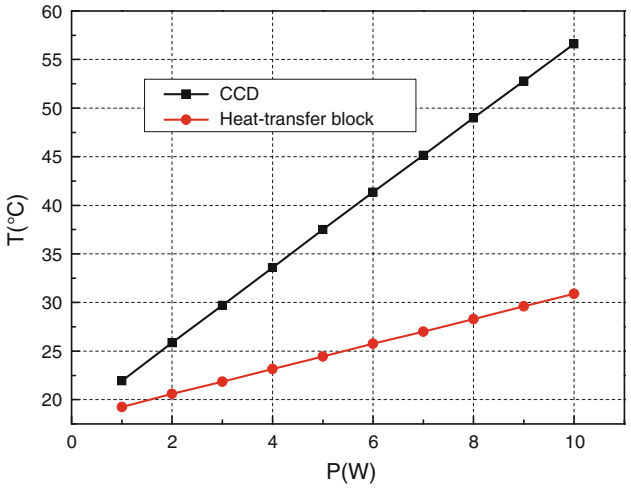

Fig. 4 The effect of inner heat source on mean temperature of FPA

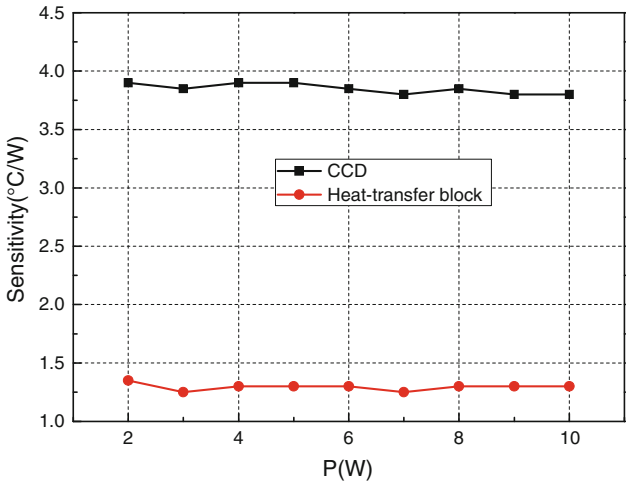

Fig. 5 The sensitivity of inner heat source on mean temperature

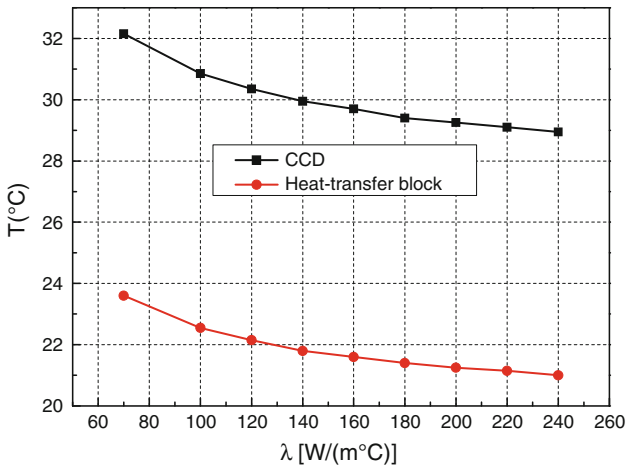

Fig. 6 The effect of material thermal conductivity on mean temperature of FPA

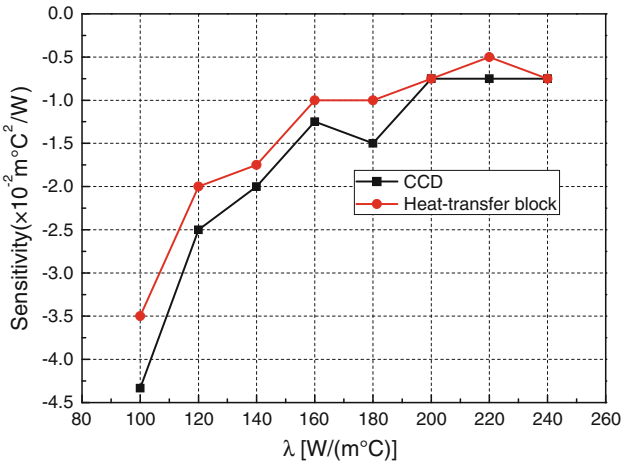

Fig. 7 The sensitivity of material thermal conductivity on mean temperature

because of the reduction of thermal resistance along heat transfer channel. The temperature uniformity and heat-sinking capability of FPA are ameliorated as the increasing of inner contact heat-transfer coefficient. The temperatures of CCD and heat-transfer block tend to be balanced after the inner contact heat-transfer coefficient attains 1,000 W/(m^2 K).

The sensitivity of inner contact heat-transfer coefficient on mean temperature in FPA is shown in the Fig. 9. The sensitivity of inner contact heat-transfer coefficient on mean temperature of CCD and heat-transfer block is -1.5×10^{-3} m^2 °C^2/W to -1.1×10^{-1} m^2 °C^2/W and -6×10^{-4} m^2 °C^2/W to -5.8×10^{-2} m^2 °C^2/W, respectively. The sensitivity of inner contact heat-transfer coefficient on CCD is higher than heat-transfer block. Under the circumstances, the inner contact heat-transfer coefficient has a greater influence on CCD than heat-transfer block.

3.4 Variation of contact heat-transfer coefficient between mounted surfaces

According to the requirement for thermal control and structural mounting in electronic device on orbit, the order of magnitude for contact heat-transfer coefficient between mounted surfaces is 10 W/(m^2 K)–10^3 W/(m^2 K). During computation process, the contact heat-transfer coefficient between mounted surfaces is set to be different number as shown in Table 2. The Other computational parameters are constant.

The effect of contact heat-transfer coefficient between mounted surfaces on mean temperature of FPA is shown in the Fig. 10. The mean temperature of CCD and heat-transfer block fall down gradually as the increasing of contact heat-transfer coefficient between mounted surfaces because of the increment of heat dissipating capacity

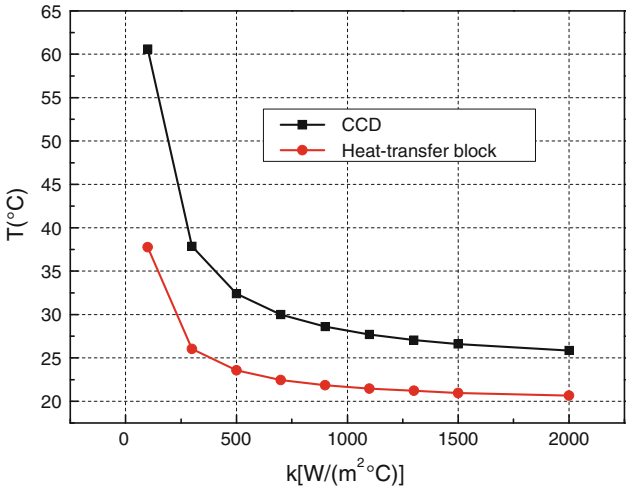

Fig. 8 The effect of inner contact heat-transfer coefficient on mean temperature of FPA

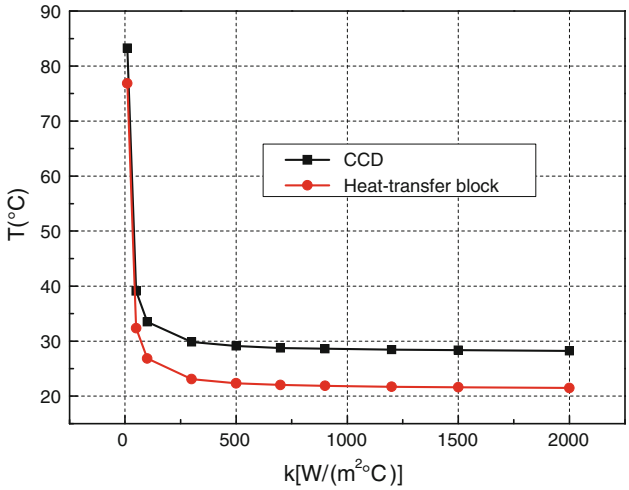

Fig. 10 The effect of contact heat-transfer coefficient between mounted surfaces on mean temperature of FPA

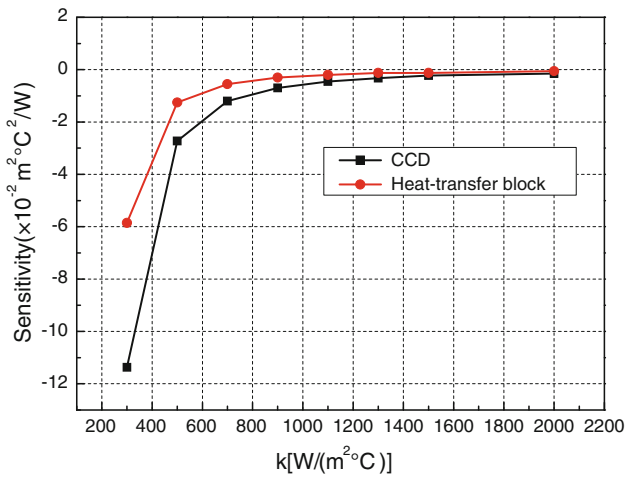

Fig. 9 The sensitivity of inner contact heat-transfer coefficient on mean temperature

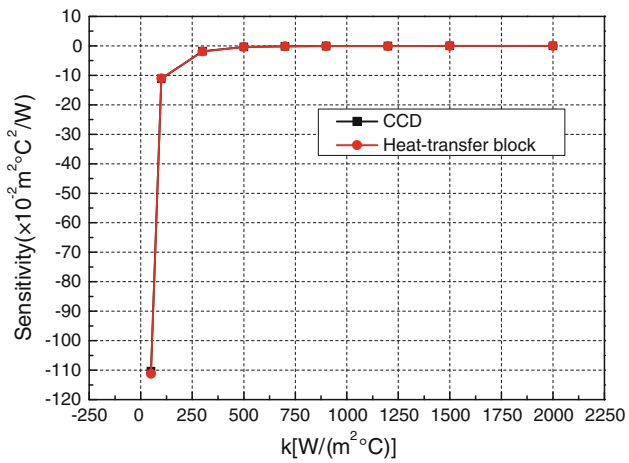

Fig. 11 The sensitivity of contact heat-transfer coefficient between mounted surfaces on mean temperature

through the mounting surface. It is obvious that the contact heat-transfer coefficient between mounted surfaces influences the temperature distribution of FPA. The temperatures of CCD and heat-transfer block tend to be balanced after the contact heat-transfer coefficient for mounted surfaces attains 500 W/(m^2 K).

The sensitivity of contact heat-transfer coefficient between mounted surfaces on mean temperature is given in the Fig. 11. The sensitivity of contact heat-transfer coefficient between mounted surfaces on mean temperature of CCD and heat-transfer block is -2×10^{-4} m^2 °C^2/W to -1.1 m^2 °C^2/W and -2×10^{-4} m^2 °C^2/W to -1.1 m^2 °C^2/W, respectively. The sensitivity of contact heat-transfer coefficient between mounted surfaces on CCD is almost the same as heat-transfer block.

3.5 Variation of surface emissivity

Generally, the surface state of FPA is anodic oxidation treatment in order to achieve a high heat-sinking capability.

During computation process, the surface emissivity is set to be different number as shown in Table 2. Heat insulation measures are put into effect on the mounted surfaces. Other computational parameters maintain constant.

The effect of surface emissivity on mean temperature of FPA is given as shown in the Fig. 12. The mean temperature of CCD and heat-transfer block decrease gradually as increasing surface emissivity under the condition of definite heat dissipating capacity through the mounted surfaces. The heat-sinking capability of FPA is improved as increasing surface emissivity.

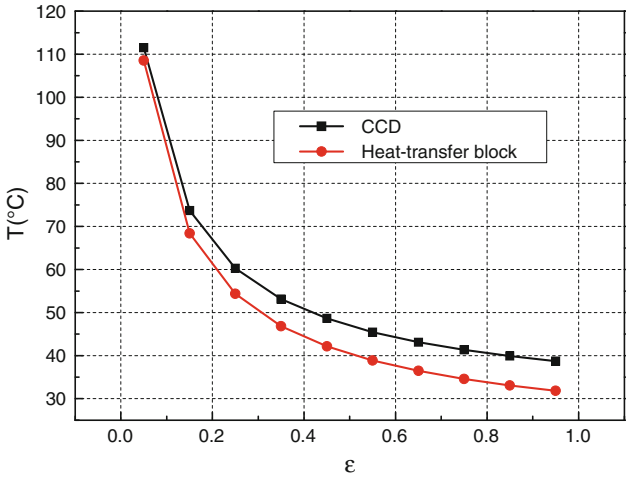

Fig. 12 The effect of surface emissivity on mean temperature of FPA

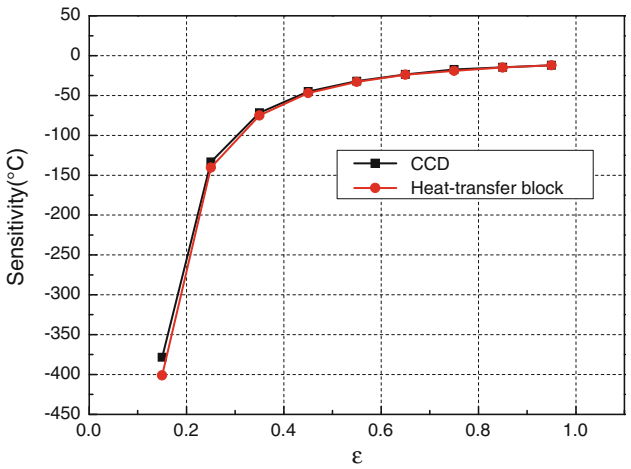

Fig. 13 The sensitivity of surface emissivity on mean temperature

The sensitivity of surface emissivity on mean temperature is shown in the Fig. 13. The sensitivity of surface emissivity on mean temperature of CCD and heat-transfer block is −12 to −378.5 °C and −12 to −401 °C, respectively. The sensitivity of surface emissivity on CCD is approximate the same as heat-transfer block. Thereby, a great attention should be paid during thermal design process for FPA, because of astringent influence of the surface emissivity on mean temperature.

3.6 Sensitivity analysis based thermal design parameters selecting

According to sensitivity analysis results mentioned above, appropriate thermal design parameters with a high sensitivity on temperature distribution of FPA could be found.

The heat generation from inner heat source has a remarkable influence on temperature distribution of FPA. Thereby, to reduce the influence of the heat productivity from inner heat source, the heat transfer measures should be enhanced, and the thermal resistance along heat transfer channel should be reduced. A great material thermal conductivity could improve temperature uniformity of FPA mostly. To satisfy requirement of temperature uniformity, the aluminum alloy 7A09 with thermal conductivity 121 W/(mK) is selected as the frame material. The inner contact heat-transfer coefficient and the contact heat-transfer coefficient between mounted surfaces are provided with important effect on reducing the temperature of CCD. The temperatures of CCD and heat-transfer block tend to be balanced after the inner contact heat-transfer coefficient and the contact heat-transfer coefficient between mounted surfaces attain 1,000 and 500 W/(m^2 K), respectively. Thereby, to reduce the influence on heat-sinking capability of FPA, heat-conducting filler such as silver foil should be filled up between the contact surfaces. As one of the thermophysical attributes, the surface emissivity is a main factor which influences temperature distribution of FPA. Thereby, to satisfy thermal design requirement, the thermal-control finishes should be with high emissivity, e.g. $\varepsilon \geq 0.85$.

4 Confirmatory test

Thermal test is an important measure to illuminate the rationality and feasibility of thermal design. The results gained in thermal test are reflection of true working situation. Furthermore, thermal test is an effective measure to verify the assumption which is made during thermal design process [36]. The drawbacks of material attribute, service load, and other initial condition and boundary condition could be given through comparison analysis with thermal test data. There will be a guide for thermal design optimization.

4.1 Test state

A mini vacuum chamber is used to simulate space environment, and the auxiliary equipments are set up to simulate surrounding environment. Including exterior surface state, heat dissipating measures and thermal control measures are put into effect as working on orbit. In course of thermal test, the temperature of heat sink, external heat flow, and running time and so on are set to be different number. The adaptive faculty of temperature for FPA is inspected. The influence of temperature level and temperature uniformity due to external surface thermophysical attribute and inner heat source and so on is verified through thermal test.

Thermal test setup is given in the Fig. 14. The external heat flow is simulated with infra-red heating setup. The temperature of mounting surface is set to be 18 °C.

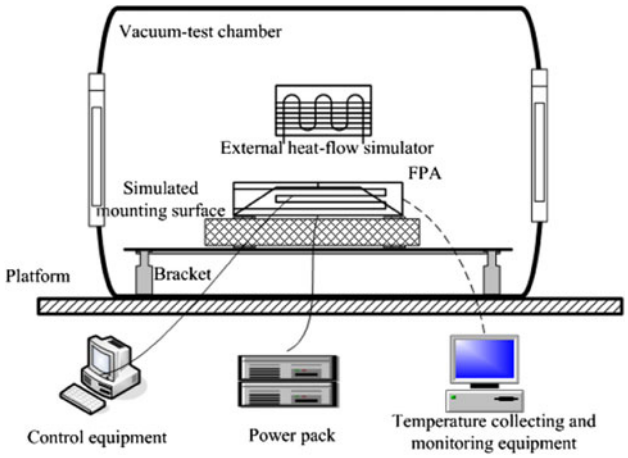

Fig. 14 Diagrammatic sketch of the thermal test instruments

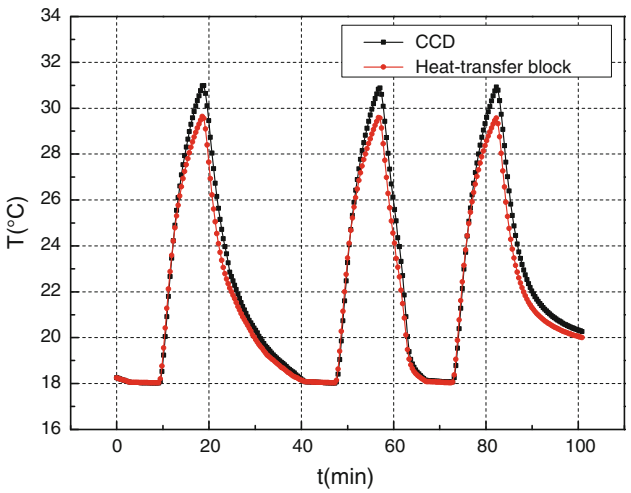

Fig. 15 Transient-state temperature curve of FPA in thermal test

4.2 Test results and analysis

According to working mode on orbit, transient-state temperature curve of FPA in thermal test is gained as shown in the Fig. 15. The temperature of CCD and heat-transfer block raises 12.7 and 11.1 °C, respectively during imaging. The highest temperature of CCD is 30.9 °C, and the highest temperature of heat-transfer block is 29.3 °C. All the temperature data satisfies the index of thermal design. It is shown that the current parameters could be selected to be the thermal design parameters. The validity and feasibility of thermal design scheme based on sensitivity analysis are verified through thermal test results.

5 Conclusions

The problem of thermal design for FPA of a space optics remote sensor is described by means of system sensitivity theory, and the on-orbit heat balance equations are established. Under the design variable analysis of the heat balance equations, thermal design parameters are given, which effect the temperature distribution of all the components. As an example, sensitivity of thermal design parameters is analyzed for FPA on a space spectral imaging instrument. Such an analysis provides a basis of structural and thermophysical parameters determination for the thermal design of a FPA in space, furthermore, provides an analytical method for reliability validation of thermal design and the operating reliability on orbit.

It is shown that the contact heat-transfer coefficient for mounted surfaces and the surface emissivity are main thermal design parameters which influence the mean temperature of CCD. The proper value selected could enhance heat-sinking capability of FPA. For CCD, the sensitivity of the contact heat-transfer coefficient for mounted surfaces on mean temperature is -2×10^{-4} m^2 °C^2/W to -1.1 m^2 °C^2/W; and the sensitivity of the surface emissivity on mean temperature is -12 to -378.5 °C. Other thermal design parameters, such as the heat productivity from inner heat source, thermal conductivity of material, and inner contact heat-transfer coefficient, influence great on the temperature difference between CCD and heat-transfer block. The proper value selected could improve temperature uniformity and temperature stability of FPA. For CCD, the sensitivity of thermal design parameters mentioned above on mean temperature is 3.8 to 3.9 °C/W, -7.5×10^{-3} m °C^2/W to -4.3×10^{-2} m °C^2/W, -1.5×10^{-3} m^2 °C^2/W to -1.1×10^{-1} m^2 °C^2/W, respectively. It is shown that the thermal design scheme based on sensitivity analysis is effective and feasible.

References

1. Guo L, Wu QW (2009) Thermal design and proof tests of CCD components in spectral imagers. Opt Precis Eng 17(10):2440–2444
2. Guo L, Wu QW, Yan CHX et al (2010) Thermal design and verification of CCD components in spectral imagers at steady and transient states. Opt Precis Eng 18(11):2375–2383
3. Anees A, Thomas A, Robert G et al (2001) Structural and thermal modeling of a cooled CCD camera. SPIE 4444:122–129
4. Kennea JA, Burrows DN, Wells A et al (2005) Controlling the swift XRT CCD temperature with passive cooling. SPIE 5898–16:1–11
5. Ding YW, Lu E (2003) Thermal design of CCD driver and its temperature changing in the course of taking picture of space remote sensor. Opt Tech 29(2):172–176
6. Zi KM, Wu QW, Guo J et al (2008) Thermal design of CCD focal plane assembly of space optical remote-sensor. Opt Tech 34(3):401–407
7. Chen ET, Lu E (2000) Thermal engineering design of CCD component of space remote-sensor. Opt Precis Eng 8(6):522–525

8. Li GQ, Jia H (2003) Thermal analysis and thermal balance test of CCD assembly. Spacecr Recovery Remote Sens 24(3):15–18
9. Luo ZHT, Xu SHY, Chen LH (2008) Thermal control of high-power focal plane apparatus. Opt Precis Eng 16(11):2187–2192
10. Zhang BQ, Ma JSH, Pan LF et al (2007) Improvement of high frequency dynamic performance of actuator in optical pickup by finite element and sensitivity methods. Opt Precis Eng 15(7): 1002–1008
11. He J, Zhou ZH, Dong HJ (2010) Design of coefficient-adjustable FBG strain sensors. Opt Precis Eng 18(11):2339–2346
12. Liu JG, Li J, Hao ZHH (2006) Study on detection sensitivity of APS star tracker. Opt Precis Eng 14(4):553–557
13. Chen BS, Gu YX, Zhang HW et al (2000) Sensitivity analysis of transient heat conduction with precise time integration method. J Mech Strength 22(4):270–274
14. Chen BS, Lin W, Gu YX (2003) Adjoint method of heat conduction sensitivity analysis. Chin J Comput Mech 20(4):383–390
15. Gu YX, Chen BS, Zhang HW et al (2002) A sensitivity analysis method for linear and nonlinear transient heat conduction with precise time integration. Struct Multidisc Optim 24:23–37
16. Colin E, Etienne S, Pelletier D et al (2005) Application of a sensitivity equation method to turbulent flows with heat transfer. Int J Therm Sci 44:1024–1038
17. Evandro PJ, João BMSJ (2008) Design sensitivity analysis of nonlinear structures subjected to thermal loads. Comput Struct 86:1369–1384
18. Dems K, Rousselet B (1999) Sensitivity analysis for transient heat conduction in a solid body-Part I: external boundary modification. Struct Optim 17:36–45
19. Dems K, Rousselet B (1999) Sensitivity analysis for transient heat conduction in a solid body-Part II: interface modification. Struct Optim 17:46–54
20. Frankel JI, Keyhani M, Huang MG (2010) Local sensitivity analysis for the heat flux-temperature integral relationship in the half-space. Appl Math Comput 217:363–375
21. Dinesh B, Subrata R (2001) Design sensitivity analysis and optimization of steady fluid-thermal systems. Comput Methods Appl Eng 190:5465–5479
22. Babak S, Chan YC (2006) Sensitivity analysis of freestream turbulence parameters on stagnation region heat transfer using a neural network. Int J Heat Fluid Flow 27:1061–1068
23. Ryszard K (2006) Sensitivity analysis and shape optimization for transient heat conduction with radiation. Int J Heat Mass Transf 49:2033–2043
24. Ryszard K (2010) Sensitivity oriented shape optimization of textile composites during coupled heat and mass transport. Int J Heat Mass Transf 53:2385–2392
25. Ding YW, Han SH, Li JH (2002) Analysis for thermo-optical sensitivity of space optical window. Opto-Electron Eng 29(5): 15–18
26. Ding YW, Wang L, You ZH et al (2005) Thermo-optical sensitivity and thermal control system for manned spaceship optical windows. J Tsinghua Univ (Sci Tech) 45(11):1489–1492
27. Lin ZHR (2006) Thermo-optical sensibility analysis of a typical R-C imaging system's primary optical equipment. Spacecr Recovery Remote Sens 27(3):17–21
28. Han YG, Xuan YM (2004) Parameter sensitivity analysis for the satellite thermal design. Chin J Comput Phys 21(5):455–460
29. Han YG, Xuan YM (2006) Parameter sensitivity analysis for the solar array of the satellite thermal design. J Nanjing Univ Sci Technol 30(2):178–181
30. Yang M, Wu XD, Lv XY et al (2010) Analysis for infrared radiation sensitivity of space satellite based on degradation of thermal control coatings. Opto-Electron Eng 37(7):30–35
31. Cho YH, Jae HY, Kyun HL et al (2011) Sensitivity analyses of satellite propulsion components with their thermal modelling. Adv Space Res 47:466–479
32. Tae HK, Dong-Kwon K, Sung JK (2009) Study of the sensitivity of a thermal flow sensor. Int J Heat Mass Transf 52:2140–2144
33. Clarke DD, Vasquez VR, Whiting WB et al (2001) Sensitivity and uncertainty analyses of heat-exchanger designs to physical properties estimation. Appl Therm Eng 21:993–1017
34. Gopi N, Michael GS, Gregory LM et al (2005) Parametric sensitivity study of operating and design variables in wellbore heat exchangers. Geothermics 34:330–346
35. Guo L, Wu QW, Yan CHX (2011) Thermal design, thermal analysis and verification in space spectral imaging apparatus. Opt Precis Eng 19(6):1272–1280
36. Li JH, Han SHL, Lu E et al (1999) Thermal analysis and thermal test in space remote-sense camera thermal control design. Opt Precis Eng 7(2):116–120